ELSEVIER

Polymer 43 (2002) 6879–6886

polymer

www.elsevier.com/locate/polymer

Effect of rigid amorphous phase on glass transition behavior of poly(trimethylene terephthalate)

Po-Da Hong[a,*], Wei-Tsung Chuang[a], Wei-Jun Yeh[a], Tsang-Lang Lin[b]

[a]*Department of Fiber and Polymer Engineering, National Taiwan University of Science and Technology, Taipei 10607, Taiwan, ROC*
[b]*Department of Engineering and System Science, National Tsing Hua University, Hsin-Chu 30013, Taiwan, ROC*

Received 30 October 2001; received in revised form 4 March 2002; accepted 20 July 2002

Abstract

In this work, a three-phase model consisting of crystalline, mobile amorphous and rigid amorphous phases (RAP) was used to describe the structural formation of poly(trimethylene terephthalate) (PTT) at various crystallization conditions. The variation in thickness and fraction of each phase was studied on both crystallization temperature T_c and crystallization time t_c effects from differential scanning calorimetry and small angle X-ray scattering analyzes. The results showed that the rigid amorphous fraction and thickness of PTT increased with increasing T_c. Meanwhile, there is no remarkable change in crystalline fraction and thickness, and long period. A characteristic length ξ_a for cooperative motion of polymer chains in amorphous phase was determined from the variation in glass transition interval using dynamic mechanical analysis. The change in this length scale of glass transition was considered to be correlated with the variation in the thickness of rigid and mobile amorphous phases. The T_g of PTT increases and the relaxation peak becomes broader at high temperature flank with T_c. These facts are considered due to that the RAP formation leads to the suppression of cooperative motion for amorphous chains.

Keywords: Poly(trimethylene terephthalate); Rigid amorphous phase; Cooperatively rearranging region

1. Introduction

Generally, the highly ordered structure of most semi-crystalline polymers could not be simply described as a conventional two-phase model consisting of crystalline and amorphous phases. Then, the third phase, the so-called 'rigid amorphous phase' (RAP) or interphase between crystalline and amorphous layers has been taken into consideration in the structure of semi-crystalline polymers. Several polymers such as poly(phenylene sulfide) (PPS) [1–5], poly(ethylene terephthalate) (PET) [6–8], poly (butylene terephthalate) (PBT) [9], poly(carbonate) (PC) [10], and poly(ether ether ketone) (PEEK) [11–13], have been found to possess of a RAP as an additional intermediate component in their structures. These facts mean that the relatively rigid polymers might easily form a RAP structure due to their poorer chain flexibility.

Recently, poly(trimethylene terephthalate) (PTT) has been introduced to the polyester family as PET and PBT. Owing to the excellent elastic recovery of PTT compared with that of PET and PBT, many structural investigations have been extensively carried out [14–26]. Wunderlich and co-workers [16,17] studied the thermal properties of PTT as a function of processing history, and they suggested that PTT might posses a RAP structure because the amorphous phase does not exhibit a rubber- or liquid-like behavior above the glass transition temperature T_g. On the other hand, the solid-state NMR results reported by Grebowicz and Chuah [27] indicated that the spin-relaxation times of PTT could not be fitted using a simple two-phase model. These results strongly indicate a RAP characteristic for PTT. Generally, the isothermal crystallization at lower temperatures would give rise to a larger rigid amorphous fraction [1,2,5,9]. However, this result is inconsistent with our present result, i.e. the rigid amorphous fraction increases as crystallization temperature is increased for PTT. More extensive studies may be necessary to make clear the effect of crystallization condition on the RAP formation.

On the other hand, it is well realized that the glass transition temperature (T_g) is highly sensitive to the

* Corresponding author. Tel.: +886-2-27376539; fax: +886-2-27376544.
E-mail address: phong@tx.ntust.edu.tw (P.D. Hong).

0032-3861/02/$ - see front matter
PII: S0032-3861(02)00617-1

crystalline morphology and amorphous structure of the material as governed by thermal history. The RAP having distinct chain mobility from liquid-like amorphous phase should relax at a temperature higher than T_g, but not at T_g, as only the relaxation of liquid-like amorphous chains takes place, resulting in a slight change in the heat capacity at T_g. Cheng et al. [5,9] have suggested that the rigid amorphous fraction does not contribute to the increase in heat capacity at T_g but unfreeze only at a higher temperature. The influence of geometrical restrictions on the glass transition of materials has generated a good idea in both experimental and theoretical studies [28–33]. Adam and Gibbs [34] proposed the size of cooperatively rearranging region (CRR) for determining the configuration restrictions in the glass-forming liquids. They defined the CRR as the smallest region that can undergo a transition to a new configuration without a requisite simultaneous conformational change on and outside its boundary. In other words, the CRR size represents a region where molecular motions in undercooled liquids are cooperatively correlated. Then they suggested that the temperature dependence of relaxation phenomena in glass-forming liquids is essentially considered in terms of the temperature dependence of the CRR size. For the case in polymers, Schick and Donth [6] reported that the effect of the CRR size is still found in the amorphous phase of crystallized PET samples. Since the relaxation process in the amorphous phase above T_g is considered related to the CRR size [30], the RAP formation may give rise to various relaxation processes of amorphous phase due to the change in the CRR size.

In this study, the effect of crystallization condition on the RAP formation for PTT was first investigated. Since RAP is considered to be located at the interphase between crystalline and mobile amorphous phases, the corresponding interphase thickness could be characterized from the small angle X-ray scattering (SAXS) method proposed by Koberstein et al. [35]. Then the differential scanning calorimetry (DSC) measurement was used to determine the rigid amorphous fraction. Finally, the RAP effect on glass transition behavior would be elucidated from the correlation with the change in the CRR size at various crystallization conditions.

2. Experimental section

2.1. Materials

PTT was kindly supplied from Industrial Technology Research Institute (ITRI), Taiwan. The PTT used in this work is obtained by the direct esterification of 1,3-propanediol (PDO) with terephthalic acid (TPA) in the melt phase with tetraisopropyl titanate as the catalyst. The intrinsic viscosity of the PTT obtained from a phenol/tetrachloroethane (60/40) mixed solution at 298 K is ca. 0.84 ml/g. According to the result reported by Chuah et al. [36], the relationship between the molecular weight and intrinsic viscosity of the PTT is $[\eta]_{\text{phenol/tetrachloroethane}} = 5.36M_n^{0.69}$. Therefore, the M_n of the PTT used can be estimated as ca. 43,000. All specimens were first dried at 363 K for 6 h under vacuum before any new thermal treatment and experimental characterization. The crystallized specimens were prepared by melting the as-received chips at 553 K for 10 min to eliminate thermal history, and then quickly cooled to a selected crystallization condition.

2.2. SAXS measurement and analysis

SAXS experiment was performed at National Tsing Hua University in Hsin-Chu, Taiwan. The graphite-monochromated Cu Kα X-ray ($\lambda = 1.524$ Å) was generated from a 18 kW Rigaku rotating anode and the power source was operated at 200 mA and 40 kV. The pinhole collimation of the X-ray beam was used. The scattered intensity was collected by a two-dimensional position sensitive detector. The data were corrected for background and detector response, and then azimuthally averaged for analysis.

SAXS is a powerful tool for the characterization of microphase structure in polymeric materials. The crystalline–amorphous structure is usually analyzed in terms of one-dimensional stack model, which the stacks consist of crystalline lamellae separated by amorphous layers, by using the one-dimensional correlation function, $\gamma(x)$ defined as follows [37]

$$\gamma(x) = \frac{1}{Q}\int_0^\infty I(q)q^2\cos(qx)\mathrm{d}q \tag{1}$$

where $I(q)$ is the scattered intensity, $q = 4\pi/\lambda\sin(\theta/2)$ (θ is the scattering angle) is the scattering vector and the scattering invariant, Q is expressed as

$$Q = \int_0^\infty Iq^2\,\mathrm{d}q \tag{2}$$

The $\gamma(x)$ is normalized by $Q(\gamma(0) = 1)$. Since SAXS data are collected in a limited angular range, it must be necessarily extrapolated to both high q and low q ranges. The extension to high q data is performed with a Porod–Ruland model [38], then the $I(q)$ can be described by

$$I(q) = K_p\frac{\exp(-\sigma^2q^2)}{q^4} + I_b \tag{3}$$

where K_p is the Porod constant, I_b is the background intensity arising from the thermal density fluctuation, and σ is related to the thickness of crystalline–amorphous interphase. The extrapolation to zero q data is obtained by fitting the intensity curve at low q range with the Deby–Bueche model [39,40]

$$I(q) = \frac{I(0)}{(1+q^2\xi^2)^2} \tag{4}$$

where ξ is the correlation length. Once the Porod constant K_p, the background intensity I_b, the interphase correction

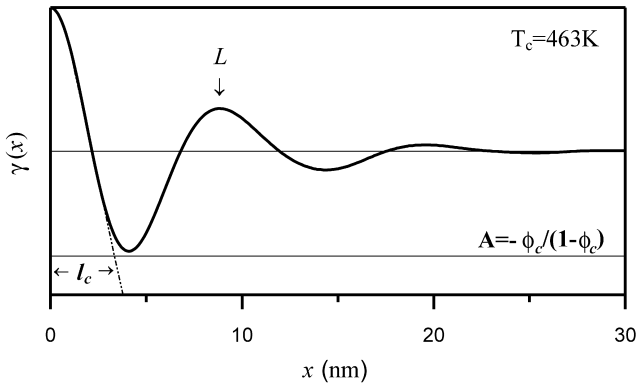

Fig. 1. Typical shape analysis of the one-dimensional correlation function and associated parameters for PTT with $\phi_c < 0.5$.

term σ, and the correlation length ξ have been estimated, the $\gamma(x)$ can be easily calculated.

The correlation function shows the electron density fluctuations at the correlation distance x and can be calculated from the Fourier transform of the observed scattered intensity on a relative scale. Fig. 1 shows a typical curve of $\gamma(x)$ for PTT crystallized at 463 K for 5 h. The shape of $\gamma(x)$ could directly yield some structural information. In the figure, the extrapolation of the linear portion of $\gamma(x)$ from small values of x to $x = 0$, the so-called 'self-correlation triangle', could yield the Q value. The base of the self-correlation triangle can be drawn as a baseline, A ($A = -\phi_c/(1-\phi_c)$ [41]), where ϕ_c is the crystallinity determined by wide-angle X-ray diffraction method as described in our previous study [42]. The correlation function is distorted by various factors such as the form of the interface, broad distributions of the crystalline thickness, and the long period; thus, the calculated $\gamma(x)$ does not reach the baseline. For this reason, the crystalline thickness l_c can be determined from an intercept of the linear portion of $\gamma(x)$

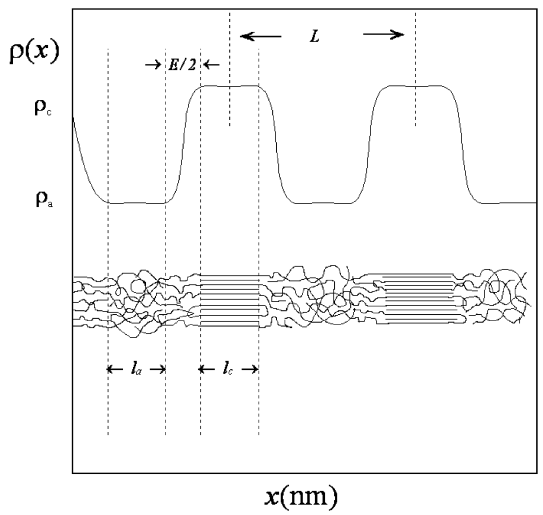

Fig. 2. Schematic representation of the electron density profile with transition range and three-phase model for PTT.

and baseline A. Further, the long period L is extracted from the position of the first maximum of $\gamma(x)$.

The interphase thickness was determined using the Porod's law based on the sigmoid gradient model. The background subtracted SAXS intensity, I_b gives Porod's law negative deviations due to the existence of the diffuse boundary region. For the pinhole SAXS intensity, it is expressed by assuming the Gaussian smoothing function for the transition range with a sigmoidal gradient model as follows (Fig. 2) [35]

$$\ln[I(q)q^4 - I_b(q)q^4] = \ln K_p - \sigma^2 q^2 \quad (5)$$

where σ is the standard deviation of the Gaussian smoothing function. The σ value contains the information of the interface thickness, e; in accordance with Eq. (5), the slope of the expected straight line will give the σ^2 variance. The half-interphase thickness e can be evaluated from [43]

$$e = \sqrt{2\pi}\sigma \quad (6)$$

where the total interphase thickness per long period E, is $2e$.

2.3. DSC measurement

DSC was carried out using a Perkin–Elmer Pyris 1 equipment. The baseline was run with a similar empty pan, using an identical method. All DSC measurements were performed from 203 to 553 K at a heating rate of 10 K/min under a dry nitrogen gas. The instrument was calibrated using standard samples of indium and zinc at the same scanning rate. In order to avoid an uneven thermal conduction through the sample, the aluminum pan was always filled with the sample weight of ca. 10 mg.

2.4. Dynamic mechanical analysis

The dynamic mechanical analysis (DMA) measurement was performed using a Perkin–Elmer DMA7 equipment. The three-point bending method was carried out at the frequency of 1 Hz and heating rate of 10 K/min in the temperature range from 270 to 450 K.

3. Results

3.1. Determination of structural parameters for crystallized PTT by SAXS

The representative result of one-dimensional correlation function $\gamma(x)$ for PTT is shown in Fig. 1. The presence of a maximum in the correlation function is indicative of a periodicity in the phase correlation, and this is often related to the average inter-domain spacing. The L value obtained from the position of the first maximum of $\gamma(x)$ that could be divided into three components, i.e. the crystal lamellar thickness l_c, mobile amorphous thickness l_a and interphase

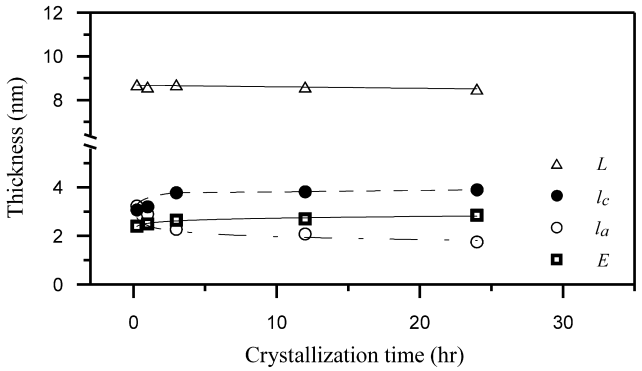

Fig. 3. The variation in structural parameters of PTT with crystallization time.

thickness E, using a three-phase model, as shown in Fig. 2. The long period L and the thickness of each phase as functions of crystallization time t_c and crystallization temperature T_c are shown in Figs. 3 and 4, respectively. The L value is almost independent of t_c and T_c, and it maintains a constant length of ca. 8.5 nm. The unchanged L value with T_c was also found in the case of PPS [44]. The l_a value decreases and the l_c and E values increase with increasing t_c, respectively. Besides, the l_c and E increments become less unobvious beyond $t_c = 3$ h. In order to investigate the T_c effect on structural change of PTT, the condition of $t_c = 5$ h was selected for isothermal crystallization at various T_cs. As the result shown in Fig. 4, the L and l_c values have no remarkable change; meanwhile, the E and l_a values change significantly with T_c. It should be mentioned here that the L value maintains a constant thickness of ca. 8.5 nm over the entire T_c range. However, the E value varies from 2.2 to 3.2 nm, i.e. the interphase thickness almost occupies the one-third part of long period, indicating that RAP is of considerable importance in the structural formation of PTT.

3.2. Determination of rigid amorphous fraction by DSC analysis

The rigid amorphous fraction permits the quantitative

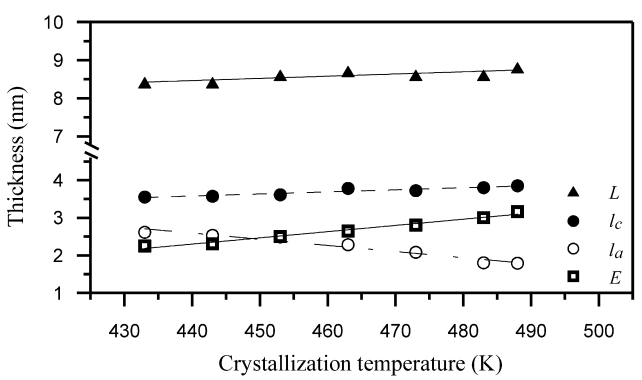

Fig. 4. The variation in structural parameters of PTT with crystallization temperature.

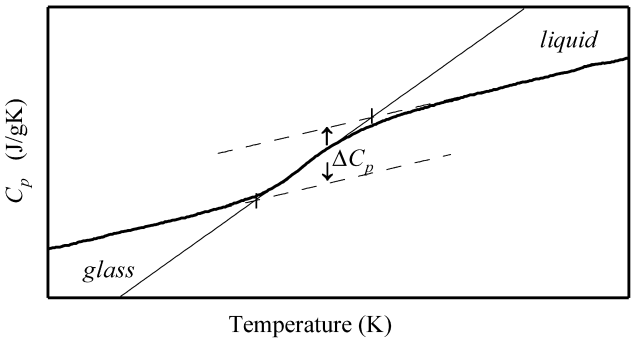

Fig. 5. Schematic DSC trace in the glass transition region; the ΔC_p = step height (distance between tangents at T_g).

characterization of linkage between crystalline and amorphous phases. A quantitative study of this phenomenon via thermal analysis was possible [5]. When a simply ideal two-phase model is valid, amorphous fraction W_a should be equal to $1 - W_c$. If $W_a < 1 - W_c$, the interphase of RAP would exist between crystalline and amorphous layers. Combining the crystalline fraction from heat of fusion and amorphous fraction from heat capacity, one can obtain an approximate estimate of RAP fraction W_{rap} from Eq. (7).

$$W_{rap} = 1 - W_a - W_c \tag{7}$$

The application of Eq. (7) in the W_{rap} estimation is limited by three-phase model and the RAP does not contribute to the increase in heat capacity at T_g but unfreezes only at a higher temperature [12]. The mobile amorphous fraction, W_a was calculated from the heat capacity increment according to

$$W_a = \frac{(\Delta C_p)_m}{(\Delta C_p)_a} \tag{8}$$

where $(\Delta C_p)_m$ is the measured heat capacity increment at T_g for PTT (Fig. 5). The heat capacity increment of mobile amorphous phase at T_g, $(\Delta C_p)_a = 94$ J/g, has been obtained

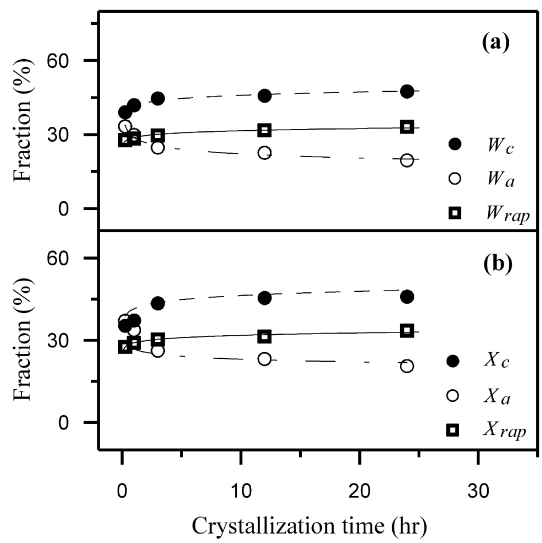

Fig. 6. The variation in the fractions of three phases with crystallization time: (a) DSC result (b) SAXS result.

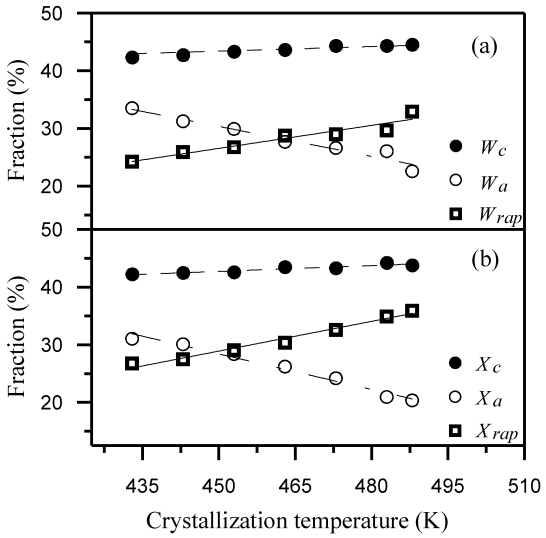

Fig. 7. The variation in the fractions of three phases with crystallization temperature: (a) DSC result (b) SAXS result.

from the DSC result reported by Pyda et al. [16]. Then W_c was determined from the ratio of ΔH_f^m and ΔH_f^0 for PTT:

$$W_c = \frac{\Delta H_f^m}{\Delta H_f^0} \tag{9}$$

The crystallinity was determined from the heat of fusion of the crystal phase from the endothermic melting peak. The ΔH_f^0 value of 28.8 kJ/mol was obtained from our previous result for PTT [42].

The fractions of each phase as functions of t_c and T_c are shown in Figs. 6(a) and 7(a), respectively. The W_a value decreases; meanwhile, the W_c and W_{rap} values increase with increasing t_c at $T_c = 463$ K. The change in these values becomes unobvious beyond $t_c = 3$ h. On the other hand, the W_c and W_{rap} values increase as T_c is increased, but the

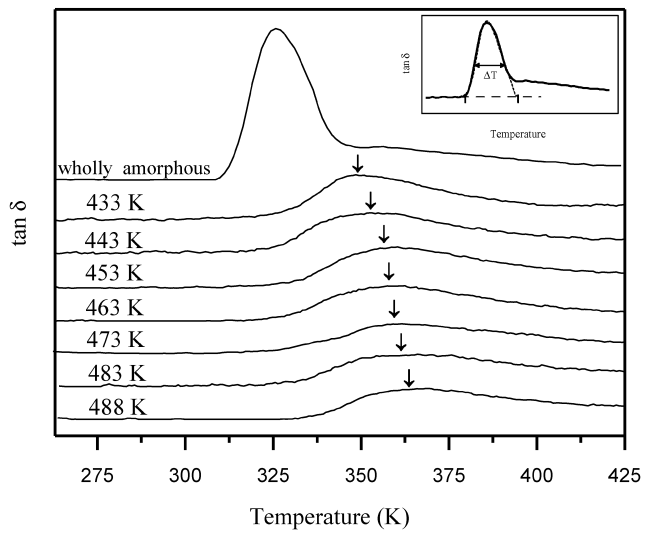

Fig. 8. Loss tan δ of PTT as a function of crystallization temperature. The insert is the determination of ΔT = full-width at half-maximum of relaxation peak.

increment of W_{rap} value with T_c is larger than that in W_c value. The result in the fraction and thickness of three phases from DSC (Figs. 6(a) and 7(a)) and SAXS analyzes (Figs. 3 and 4) shows a similar tendency. In order to compare the fraction of each phase from the DSC result with SAXS result, we make a reasonable assumption on total crystalline lamellae distributed alternately with amorphous layers in the present work. In some cases better agreement with SAXS data is obtained if the presence of a transition phase boundary is assumed. Based on this assumption, a linear dependence on distance of electron density distribution is schematically shown in Fig. 2. It could also represent the structure of a unoriented semi-crystalline polymer with an ensemble of densely packed and isotropically distributed stacks of parallel lamellae [37]. Thus, the SAXS data could be used to compute the linear fraction of crystalline phase, mobile amorphous phase and interphase using the following relation

$$X_c = l_c/L; \qquad X_a = l_a/L; \qquad X_{rap} = E/L \tag{10}$$

where X_c, X_a and X_{rap} are the linear fractions of crystalline, mobile amorphous and interphase fractions, respectively. The linear fractions as functions of t_c and T_c are, respectively, shown in Figs. 6(b) and 7(b). The values of interphase fraction from SAXS are very close to those of bulk rigid amorphous fraction obtained from DSC analysis, indicating that the RAP evidently exists between two adjacent crystal lamellae for crystallized PTT in this work. Regarding the T_c effect, the increment of W_{rap} or X_{rap} was much higher than increment of W_c or X_c, indicating that RAP formation must play a significant role during isothermal crystallization.

3.3. CRR size effect on glass transition temperature of PTT

Fig. 8 shows the mechanical loss tangent tan δ as a function of T_c for PTT. The peak in tan δ spectrum is defined as the α relaxation process and the peak temperature is T_g. As T_c is increased, the distribution of α relaxation gradually becomes broader and the T_g shifts to high temperature from 350 to 370 K. By restricting the molecular motion in glassy material, there may be an interference with the spatial extent of cooperativity [28–33]. Donth [30] suggested that the effect of cooperativity size, i.e. the size of the CRR proposed by Adam and Gibbs [26], still exists in the amorphous phase of semi-crystalline polymers. Then, the CRR size could be estimated from the mean temperature fluctuation of the cooperative subsystems δT according to [30]

$$V_a = \frac{k_B T_g^2}{(\Delta C_p)_m (\delta T)^2 \rho} \tag{11}$$

where ρ is the bulk density (ca. 1.38 g/cm^3) for PTT [45], k_B is the Boltzmann constant, V_a is the mean volume of one CRR, and $(\Delta C_p)_m$ is the measured heat capacity increase at

Table 1
The parameters related to glass transition of PTT crystallized at various T_cs

T_c (K)	T_g (K)	ΔT (K)	V_a (nm^3)	ξ_a (nm)
433	349	41	19.2	1.53
443	352	44	18.7	1.49
453	359	46	18.5	1.48
463	360	49	17.7	1.41
473	362	52	17.4	1.38
483	363	55	15.8	1.26
488	365	60	15.0	1.20
Wholly amorphous	325	26	22.6	1.80

T_g ($(\Delta C_p)_m$ in J/g K). The δT could be directly determined from the glass transition interval ΔT obtained from a thermogram: $2\delta T \approx$ width of the glass transition interval measured in temperature units [30]. In the present study, we determined the glass transition interval ΔT from the distribution of tan δ peak, i.e. the full-width at half-maximum as shown in Fig. 8. The characteristic length ξ_a is the corresponding radius of the cooperativity region characterized by the volume V_a.

$$\xi_a = \left(\frac{3V_a}{4\pi}\right)^{1/3} \tag{12}$$

Combining Eqs. (11) and (12), the width of the glass transition interval is inversely connected to the ξ_a value, i.e. the smaller ξ_a is due to the broader ΔT. The T_g, ΔT, V_a and ξ_a values at various T_cs for PTT are summarized and listed in Table 1. The ξ_a value is obviously decreased from 1.53 to 1.20 nm with increasing T_c, and the ξ_a value of wholly amorphous PTT is 1.8 nm. On the other hand, the increases in T_g and ΔT values are also found as T_c is increased. The ξ_a value is cooperatively correlated with the length scale of molecular motions in undercooled liquids; thus, the RAP formation in amorphous layer may induce a change in the ξ_a value, resulting in the variation of T_g and ΔT. The further discussion will be stated in Section 4.

Fig. 9 shows the DSC result at a heating rate of 10 K/min for wholly amorphous PTT prepared from quick quenching of the melt specimen by liquid nitrogen. A clear glass transition temperature is found at ca. 318 K and the total

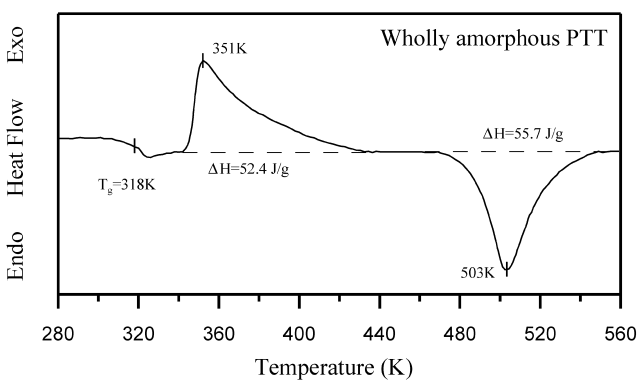

Fig. 9. DSC scan of wholly amorphous of PTT.

exothermic enthalpy of crystallization is almost the same with the melting enthalpy, indicating this starting material is completely amorphous indeed. As compared with the tan δ result of wholly amorphous PTT in Fig. 8, the T_g (peak temperature) value of ca. 325 K is higher than that in DSC result. Since the ξ_a value is cooperatively correlated with the length scale of molecular motions in amorphous phase, the T_g value determined from DMA is relatively suitable to be correlated with the physical meaning of the ξ_a value in this work.

4. Discussion

Generally, the RAP formation is very sensitive to the conditions of thermal treatment such as t_c and T_c. The t_c effect on the RAP formation may be related to the densification of mobile amorphous phase, resulting in an increase of the rigid amorphous thickness or fraction (Figs. 3 and 6). Both mobile and rigid amorphous chains may change their conformations little by little to be incorporated into crystalline phase with increasing t_c. It is generally realized that the mobile amorphous chains could not be directly incorporated into crystalline phase. A transitional phase (RAP in this work) should be first formed before crystallization. This phenomenon may be considered as a memory effect, which must then be connected to the conformational change in the mobile amorphous phase induced by the secondary crystallization process. Regarding the T_c effect (the results as stated in Figs. 4 and 7) on RAP formation, the interphase thickness and rigid amorphous fraction lineally increase with T_c. These results in PTT are inconsistent with those reported in other semi-crystalline polymers such as PEEK [11,12], PPS [1,2,4,5], i.e. the lower T_c would form less perfection of crystal to increase RAP fraction, and longer t_c or annealing time would turn RAP into crystalline phase to decrease RAP fraction. Due to the experimental facts in this work, i.e. the higher T_c the larger interphase thickness and rigid amorphous fraction for PTT, it is naturally considered that the higher chain mobility at high T_c may easily overcome the activity energy for conformational change of amorphous chains to induce the densification in mobile amorphous phase, resulting in the increase of rigid amorphous fraction and interphase thickness. It should be mentioned here that the crystalline thickness and fraction for PTT have no remarkable change with increasing T_c, indicating that the RAP cannot be easily incorporated into the crystalline phase.

In general, the relaxation of glass transition would be broadened and shifted to high temperature as the crystallinity is increased because of the reduction of chain mobility in the amorphous phase due to the confined effect in conventional two-phase model [46]. In three-phase model, the RAP should also play a role of this restricted effect of polymer chains. Combining the results in Figs. 4, 7 and 8, the T_g indeed increases with increasing interphase thickness

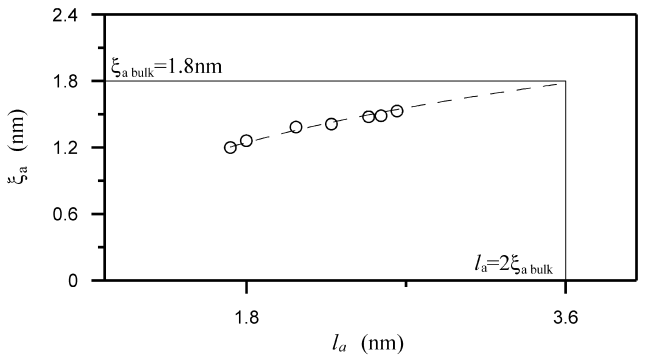

Fig. 10. The CRR size ξ_a as a function of mobile amorphous thickness l_a.

and rigid amorphous fraction. Furthermore, the ξ_a value decreases with increasing interphase thickness E. All these facts strongly suggest that the glass transition behavior is significantly affected by the RAP formation. To take into account the three-phase model, the glass transition behavior reflects the cooperative motion of polymer chains which occurred in mobile amorphous phase and squeezed in both sides of RAP (Fig. 2). This phenomenon is like a 'cage', which is large enough to allow the conformational transition of local chains. Schick and Donth [6] have also proposed a stack model consisting of crystalline, interfacial and amorphous layers for semi-crystalline polymers such as PET by considering a squeezing-in effect between self-organized structures of the substance. They suggested that the glass transition can be observed in both undisturbed bulky amorphous region with sufficiently larger size ($>2\xi_a$) and amorphous layers inside the stacks with thickness d_a (l_a in this work) $\sim \xi_a$. From the results in crystallized PET at various crystallization regions, the spatial limitation by interfacial layers indicates a direct effect of the ξ_a value on the glass transition. This interfacial layer might be considered to be consistent with the definition of the RAP structure in this work. The relationship between CRR size ξ_a and mobile amorphous thickness l_a of PTT was shown in Fig. 10. All PTT samples prepared from various crystallization temperatures show a l_a variation between 1.7 and 2.6 nm, i.e. $l_a < 2\xi_a$, where $\xi_a = 1.8$ nm for the bulky amorphous sample. The increase in l_a value is accompanied

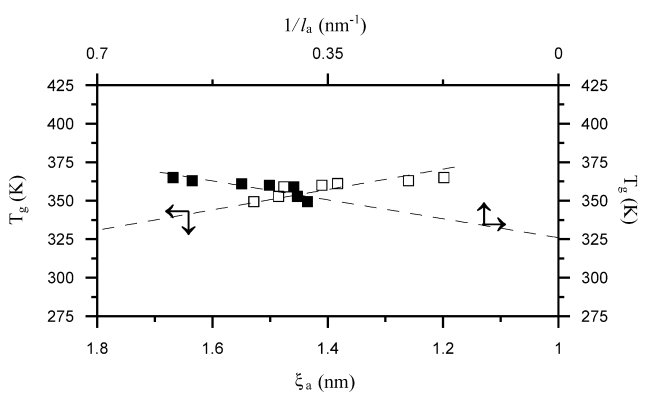

Fig. 11. Plot of T_g as functions of $1/l_a$ and ξ_a.

by the decrease in interphase thickness, because the long period and crystal thickness have no remarkable change with crystallization temperature in this work.

Since the correlation length ξ_a characterizes a region where molecular motion in amorphous phase, the RAP formation should directly give rise to the suppression of cooperative motion, leading to a broadening and temperature shift of the glass transition. Fig. 11 shows the T_g of PTT as functions of ξ_a and $1/l_a$ values, respectively. The T_g linearly decreases and increases with increasing ξ_a and $1/l_a$ values. The linear decrease of T_g with ξ_a extrapolated to $\xi_{a\,bulk} = 1.8$ nm could determine T_g = ca. 328 K for wholly amorphous PTT. On the other hand, the linear relation between T_g and $1/l_a$ could also obtain T_g = ca. 325 K as $1/l_a = 0$, i.e. $l_a = \infty$. Both ways to determine T_g of amorphous PTT were very close to that from DMA result as shown in Fig. 8. The RAP formation influences the CRR volume V_a and then it restricts cooperative motion of amorphous chains, leading to the broadening of T_g at the high temperature flank and the shift of T_g to high temperature (Fig. 8). The broadening of glass transition interval might be considered due to the interfacial heterogeneity of crystallite, i.e. loops, cilia, loose folds and inter-crystalline links, which would benefit the development of RAP. Generally, the change in interphase thickness and rigid amorphous fraction with T_c would lead to positive or negative shift of T_g. Although, Cheng et al. [5,12] and Huo and Cebe [2,4,11] reported that T_gs of PPS and PEEK decrease with T_c according to negative shift, because RAP is gradually incorporated into the crystalline phase with increasing T_c, leading to a decrease in RAP fraction. The present study reveals an evidence that both interphase thickness and rigid amorphous fraction increase with T_c because of the densification in mobile amorphous phase, i.e. the reduction of CRR size, resulting in a positive shift of T_g.

5. Conclusions

In this work, the RAP formation was taken account of structural change in PTT at various crystallization conditions. Then the interphase thickness and fraction are estimated from SAXS and DSC analyzes, respectively. The t_c effect on the RAP formation may be related to the densification of mobile amorphous phase, resulting in an increase of the interphase thickness and rigid amorphous fraction. However, the change in these values becomes unobvious beyond $t_c = 3$ h. Regarding the T_c effect on the RAP formation, the interphase thickness and rigid amorphous fraction lineally increase with T_c. The higher chain mobility at high T_c may easily overcome the activity energy for conformational change of amorphous chains to induce the densification in mobile amorphous phase, resulting in the increase of interphase thickness and rigid amorphous fraction. A characteristic CRR size, ξ_a representing a correlation length for cooperative motion of polymer chains

in amorphous phase increases with decreasing mobile amorphous thickness l_a. The decrease in l_a value should be accompanied by the increase in interphase thickness, because the long period and crystal thickness have no remarkable change with T_c in this work. The RAP formation should directly give rise to the suppression of cooperative motion, leading to a broadening and temperature shift of the glass transition.

Acknowledgements

The authors are indebted to Dr H. Chuah of Shell Company for many delightful discussions in this work. We also appreciate Dr W.C. Liu at National Tsing Hua University for technical support of SAXS measurement.

References

[1] Toshihiko J, Shigeo A, Masao S. J Macromol Sci, Phys B 1997;36:381.
[2] Huo P, Cebe P. Colloid Polym Sci 1992;270:840.
[3] Lu SX, Cebe P. Polymer 1996;37:4857.
[4] Huo P, Cebe P. J Polym Sci, Part B: Polym Phys 1992;30:239.
[5] Cheng SZD, Wu ZQ, Wunderlich B. Macromolecules 1987;20:2802.
[6] Schick C, Donth E. Phys Scripta 1991;43:423.
[7] Schick C, Wigger J, Mischok W. Acta Polym 1990;41:137.
[8] Takayanagi M, Yoshino M, Minami S. J Polym Sci 1962;61:s7.
[9] Cheng SZD, Pan R, Wunderlich B. Makromol Chem 1988;189:2443.
[10] Laredo L, Grimau M, Müllier A, Bello A, Suarez N. J Polym Phys, Part B 1996;34:2863.
[11] Huo P, Cebe P. Macromolecules 1992;25:902.
[12] Cheng SZD, Cao MY, Wundelich B. Macromolecules 1986;19:1868.
[13] Kalika DS, Krishnaswamy RK. Macromolecules 1993;26:4252.
[14] Kim KJ, Bae JH, Kim YH. Polymer 2001;42:1023.
[15] Ziabicki A, Sajkiewicz P. Colloid Polym Sci 1998;276:680.
[16] Pyda M, Boller A, Grebowicz J, Chuah HH, Lebedev BV, Wunderlich B. J Polym Sci, Part B: Polym Phys 1998;36:2499.
[17] Pyda M, Wunderlich B. J Polym Sci, Part B: Polym Phys 2000;38:622.
[18] Oppermann W, Hirt P, Fritz C. Chem Fibers Int 1999;49:33.
[19] Ho RM, Ke KZ, Chen M. Macromolecules 2000;33:7529.
[20] Wang B, Li CY, Hanzlicek J, Cheng SZD, Geil PH, Grebowicz J, Ho RM. Polymer 2001;42:7171.
[21] Yang J, Sidoti G, Liu J, Geil PH, Li CY, Cheng SZD. Polymer 2001;42:7181.
[22] Wu J, Schultz JM, Samon JM, Pangelinan AB, Chuah HH. Polymer 2000;42:7141.
[23] Grebowicz JS, Brown H, Chuah HH, Olvera JM, Wasiak A, Sajkiewicz P, Ziabicki A. Polymer 2001;42:7153.
[24] Wu J, Schultz JM, Samon JM, Pangelinan AB, Chuah HH. Polymer 2001;42:7161.
[25] Jang SS, Jo WH. J Chem Phys 1999;110:7524.
[26] Yang JS, Jo WH. J Chem Phys 2001;114:8159.
[27] Grebowicz J, Chuah HH. Progress Report. Shell Chemical Company; 1996.
[28] Sappelt D, Jäckle J. J Phys A: Math Gen 1993;26:7325.
[29] Awschalom DD, Warnock J. In: Klafter J, Drake JM, editors. Molecular dynamics in restricted geometries. New York: Wiley; 1989.
[30] Donth E. J Non-Cryst Solids 1982;53:325.
[31] Zhang J, Liu G, Jonas J. J Phys Chem 1992;96:3478.
[32] Jackson CL, Mckenna GB. J Non-Cryst Solids 1991;131–133:221.
[33] Mel'nichenko YB, Schüller J, Richert R, Ewen B. J Chem Phys 1995;103:2016.
[34] Adam G, Gibbs JH. J Chem Phys 1965;43:139.
[35] Koberstein JT, Morra B, Stein RS. J Appl Crystallogr 1980;13:34.
[36] Chuah HH, Lin VD, Soni U. Polymer 2001;42:7137.
[37] Strobl GR, Schneider M. J Polym Sci, Part B: Polym Phys 1980;18:1343.
[38] Ruland WJ. J Appl Crystallogr 1971;4:70.
[39] Deby P, Bueche AM. J Appl Phys 1949;20:518.
[40] Deby P, Anderson Jr. HR, Brumberger H. J Appl Phys 1957;28:679.
[41] Wang J, Alvarez M, Wanjin Z, Wu Z, Li Y, Chu B. Macromolecules 1992;25:6943.
[42] Chung WC, Yeh WJ, Hong PD. J Appl Polym Sci 2002;83:2426.
[43] Siemann U, Ruland W. Colloid Polym Sci 1982;260:999.
[44] D'ilario L, Piozzo A. J Mater Sci Lett 1989;8:157.
[45] Poulin-Dandurand S, Perez S, Revol J, Brisse F. Polymer 1979;20:419.
[46] Gibbs JH, DiMarzio EA. J Chem Phys 1958;28:373.